

Supporting Information

Facile synthesis of Fe-baicalein nanoparticles for photothermal/chemodynamic therapy with accelerated Fe^{III}/Fe^{II} conversion

Zhendong Liu,^{ab} Chunling Hu,^{ab} Sainan Liu,^{ab} Lihan Cai,^{ab} Ying Zhou,^a and Maolin Pang^{*ab}

^aState Key Laboratory of Rare Earth Resource Utilization, Changchun Institute of Applied Chemistry, Chinese Academy of Science; Changchun 130022, PR China.

^bUniversity of Science and Technology of China, Hefei 230026, PR China.

* Corresponding author.

E-mail address: mlpang@ciac.ac.cn.

Experimental Section

Materials: Iron (II) sulfate heptahydrate ($\text{FeSO}_4 \cdot 7\text{H}_2\text{O}$, AR, Beijing Chemical Works), Baicalein (Ba, $\text{C}_{15}\text{H}_{10}\text{O}_5$, Aladdin), Polyethylene glycol-2000 (PEG-2000, $\text{H}(\text{OCH}_2\text{CH}_2)_n\text{OH}$, Tianjin Huadong Reagent Factory), Ethanol (AR, Beijing Chemical Works), and Deionized water (Millipore, $18.2 \text{ M}\Omega \cdot \text{cm}$ resistivity at 25°C), all chemicals and chemical reagents were used directly without any further purification.

Characterization: Powder X-ray diffraction (PXRD) measurements were performed on Rigaku MiniFlex 600 at a scanning rate of $10^\circ/\text{min}$ in the 2θ range from 3 to 40° , with graphite monochromatized $\text{Cu K}\alpha$ radiation ($\lambda = 0.15405 \text{ nm}$). The morphology of the samples was characterized by using a field-emission scanning electron microscope (FE-SEM, S-4800, Hitachi) equipped with an energy-dispersive X-ray (EDX) spectrometer. Transmission electron microscopy (TEM) images were obtained on a FEI Tecnai G2 S-Twin with a field emission gun operating at 200 kV . Thermogravimetric analysis (TGA) data were recorded with Thermal Analysis Instrument (SDT 2960, TA Instruments, New Castle, DE) with a heating rate of $10^\circ\text{C}/\text{min}$ in a nitrogen flow of $100 \text{ mL}/\text{min}$. Fourier transform infrared spectra were measured on a Vertex PerkinElmer 580BIR spectrophotometer (Bruker) with KBr pellet technique. The UV-vis adsorption spectra were measured on a Hitachi U-3100 spectrophotometer. Inductively Coupled Plasma (ICP) was taken on an iCAP 6300 of Thermo scientific. The X-ray photoelectron spectra (XPS) were taken on a VG ESCALAB MK II electron energy spectrometer using Mg KR (1253.6 eV) as the X-ray excitation source. The spectra of all interested elements were referenced to the $\text{C } 1\text{s}$ peak arising from adventitious carbon (its binding energy was set at 284.6 eV). MTT experiments were carried out using a microplate reader (Thermo Multiskan MK3).

Synthesis of Fe-BaP: Fe-BaP was prepared by a simple one-pot approach. The $\text{FeSO}_4 \cdot 7\text{H}_2\text{O}$ aqueous solution (6.2 mg mL^{-1} , 1 mL) was added to the PEG-2000 solution (40 mg mL^{-1} , 3 mL) under mild stirring for 1 h . Baicalein (6 mg) was dissolved in absolute ethanol (6 mL), then added it dropwise into the above mixture solution and stirred overnight at room temperature. The black precipitates were centrifuged and washed with ethanol for three times.

Observation and Measurement of $\cdot\text{OH}$ Generation: Methylene blue (MB) was used to detect $\cdot\text{OH}$. Typically, MB aqueous solution, H_2O_2 ($100 \mu\text{M}$), and Fe-BaP aqueous solution were mixed, and then, the supernatant was collected by centrifugation, and the absorption wavelength around 660 nm was monitored by ultraviolet–visible spectroscopy. As controls, the ultraviolet–visible spectroscopy of pure MB and the mixture of MB and H_2O_2 were also monitored for comparison. Moreover, the roles of temperature and concentration of CFAP on the production of $\cdot\text{OH}$ were evaluated.

Fe^{2+} detection: 1,10-phenanthroline was used to detect reduced Fe^{2+} . $\text{FeSO}_4 \cdot 7\text{H}_2\text{O}$ (0.6 mg mL^{-1} , 1 mL), baicalein ethanol solution (0.1 mg mL^{-1} , 0.75 mL) and 1,10-phenanthroline ethanol solution (1 mg mL^{-1} , 0.75 mL) were mixed for 30 min , then replacing the Fe^{3+} in the above mixed solution with Fe^{2+} (20.6 mg mL^{-1} , 1 mL) for comparison. The absorbance could be measured by UV-Vis spectrophotometry at 508 nm .

The photothermal conversion efficiency of Fe-BaP: The photothermal conversion efficiency of Fe-BaP was calculated by previously reported literature.

$$\eta = \frac{hs(T_{max} - T_{sur}) - Q_{Dis}}{I(1 - 10^{-A_{808}})}$$

Where h is the heat transfer coefficient, S is the surface area between container and environment, T_{max} is the maximum temperature of Fe-BaP nanoparticles in the aqueous solution. T_{sur} is the environment temperature. Q_{Dis} is the heat dissipation by the test cell. I is the 808 laser power (1.3 W cm^{-2}). A_{808} is the absorbance of the Fe-BaP nanoparticles at 808 nm.

$$hs = \frac{m_d C_d}{\tau_s}$$

Where the m_d is the mass (1 g) and the C_d is the heat capacity (4.2 J/g) of the aqueous solution, τ_s is the sample system time constant.

Cell toxicity test: The biocompatibility and cytotoxicity of Fe-BaP was evaluated using a standard [3-(4,5-dimethylthiazol-2-yl)-2,5-diphenyltetrazolium bromide] (MTT) test. L929 cells were placed in a 96-well plate with a density at 6×10^3 cells per well, and incubated in RPMI for 24 h. The original medium was then sucked out and the new medium containing different concentrations of Fe-BaP was added again. After the cells were incubated for another 24 h, the medium inside was again discarded and readded with fresh RPMI containing 10 μL of the standard methyl thiazolyl tetrazolium (MTT). After placing the plates in the dark for 4 h, 150 μL of DMSO was added to each well and the absorption value of the medium was measured by a microplate reader at the wavelength of 490 nm.

To study the in vitro CDT and PTT effect of Fe-BaP, four groups of 4T1 cells were seeded into 96-well plates with a density of 6×10^3 cells per well and cultured in RPMI for 24 h. The original medium was then sucked out and the new medium containing different concentrations of Fe-BaP was added again, respectively. After the cells were incubated for 6 h, the medium inside was again discarded and readded with fresh RPMI. One group of 4T1 cells were not irradiated and the other three groups of 4T1 cells were treated with 100 μM H_2O_2 , 808 nm laser (1.3 W cm^{-2}) irradiation and a combination of 100 μM H_2O_2 and 808 nm laser (1.3 W cm^{-2}) irradiation, respectively. The cells were beamed with the laser for 5 min. Then the cells were incubated for another 24 h before the MTT assay was used to detect the cell viability.

Preparation of Rhodamine B-conjugated Fe-BaP NPs (Fe-BaP-RhB): In order to study the intracellular uptake of Fe-BaP, rhodamine B (RhB)-loaded Fe-BaP was prepared. Firstly, 10 mg of 1-(3-Dimethylaminopropyl)-3-ethylcarbodiimide hydrochloride (EDC), 3 mg of N-Hydroxysuccinimide (NHS) and 5 mg of rhodamine were dissolved in 2.5 mL of deionized water, stirring at room temperature for 1 h, and then 5 mL of Fe-BaP solution in deionized water (about 5 mg) was added and stirred overnight. The product was washed with deionized water until the supernatant was nearly colorless.

Cellular uptake of the Fe-BaP NPs: The 4T1 cells were seeded into 12 well at a density 6×10^4

per plate, and then incubated with Fe-BaP-RhB for 1, 4, and 6 h, respectively. After that, washing with PBS two times, fixed with 4% paraformaldehyde for 10 min in the dark and then stained with Hoechst 33342. The cells uptake process was monitored by intracellular fluorescence microscope.

Intracellular ROS Detection: The 4T1 cells were incubated with RPMI and RPMI containing Fe-BaP ($75 \mu\text{g mL}^{-1}$) for 24 h. Then the 4T1 cells were assigned to 7 groups to culture with RPMI-containing the following conditions: (1) control, (2) 808 nm NIR irradiation only, (3) $100 \mu\text{M H}_2\text{O}_2$ only, (4) $75 \mu\text{g mL}^{-1}$ Fe-BaP NPs only, (5) a mixture of $100 \mu\text{M H}_2\text{O}_2$ and $75 \mu\text{g mL}^{-1}$ Fe-BaP NPs, (6) $75 \mu\text{g mL}^{-1}$ Fe-BaP NPs under 808 nm NIR irradiation, (7) $75 \mu\text{g mL}^{-1}$ Fe-BaP NPs plus $100 \mu\text{M H}_2\text{O}_2$ under 808 nm NIR irradiation. After being incubated for 1 h, the cells were beamed with the laser (5 min, 1.3 W cm^{-2}). Then the culture medium was replaced and RPMI containing DCFH-DA ($10 \times 10^{-6} \text{ M}$) was added and further incubated in the dark for 20 min. Then it was washed by PBS for three times and observed under a fluorescence microscope.

Flow cytometry measurements: The 4T1 cells were seeded into 6 well at a density 2×10^5 per well, and then treated with (a) PBS; (b) NIR; (c) Fe-BaP; (4) NIR+Fe-BaP, respectively. All the cells were incubated for 12 h at 37°C , and then the 4T1 cells was washed with PBS for two times and digested with trypsin and handled with PBS (4°). The cells were stained by Annexin V-fluorescein isothiocyanate (Annexin V-FITC) and propidium iodide (PI), and then cell apoptosis rate was measured by a FACS Calibur flow cytometer (BD Biosciences).

In vivo antitumor efficacy of Fe-PAP: Female Balb/C mice were purchased from the Center of Experimental Animals, Jilin University (Changchun, China), and all the experimental mice were treated with the protocol approved by the Institutional Animal Care and Use Committee of Jilin University. The 4T1 tumor models were successfully established by subcutaneous injection of 4×10^6 cells suspended in $100 \mu\text{L}$ of phosphate buffered saline (PBS) into the right flank of each mouse. After the tumor volume reached $80\text{-}100 \text{ mm}^3$, the mice were randomly divided into 4 groups ($n=5$, per group), and treated with (PBS), PBS + NIR, Fe-BaP and Fe-BaP + NIR, respectively. For PBS + NIR and Fe-PAP + NIR groups, the tumor was irradiated with an 808 nm laser for 5 min (1.3 W cm^{-2}). Body weight and tumor size were monitored every two days for two weeks. The tumor volume was calculated by $V = 4/3 \times \text{Length} \times \text{width}^2/8$. The relative tumor volume was calculated as V/V_0 , where V_0 was the tumor volume before the treatment. Finally, the major organs of mice, such as liver, spleen, heart, lung, and kidney, were removed and fixed in 4% paraformaldehyde solution for histological examination to further investigate the biocompatibility of Fe-BaP.

In Vivo Biodistribution of Fe-BaP NPs: To determine the biodistribution of Fe-BaP NPs, mice after injection with Fe-BaP NPs, major organs and tissues (heart, liver, spleen, lung kidney, and tumor) from Balb/c mice ($n = 3$) were collected at a certain time interval. Next, the collected organs were wet-weighted and dissolved in chloroazotic acid under heating at 60°C for 12 h. After each sample was diluted with deionized water to 10 mL , ICP - MS was used to measure Fe concentrations in different samples.

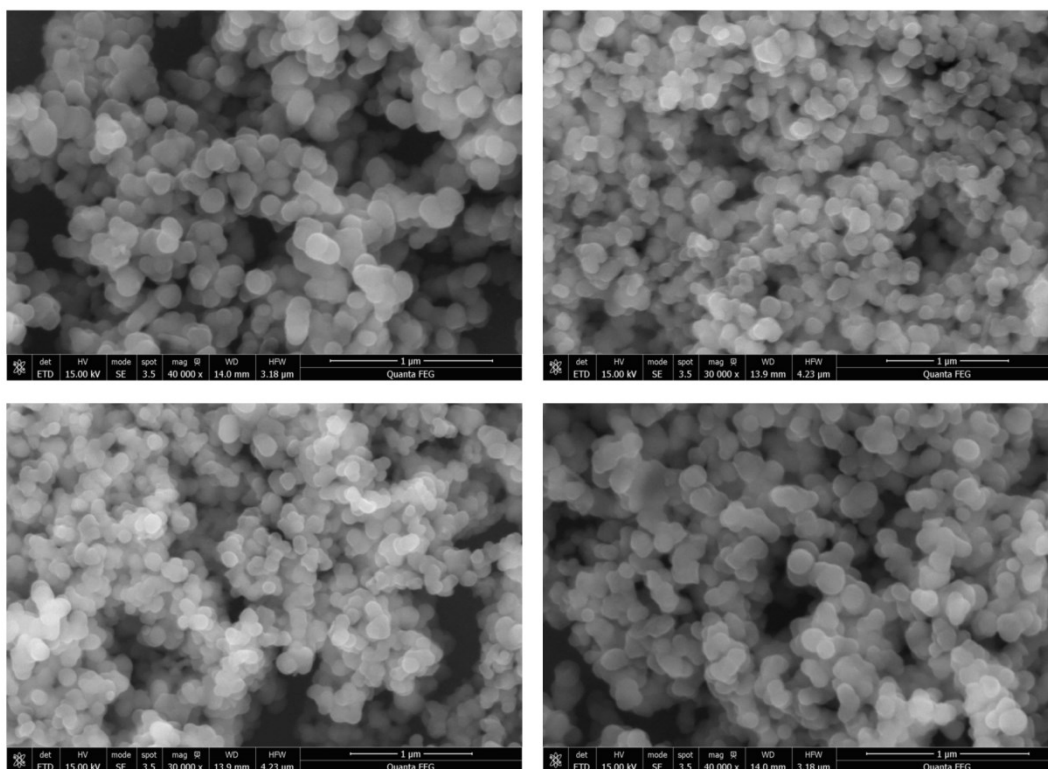


Fig. S1 Additional SEM images of Fe-BaP.

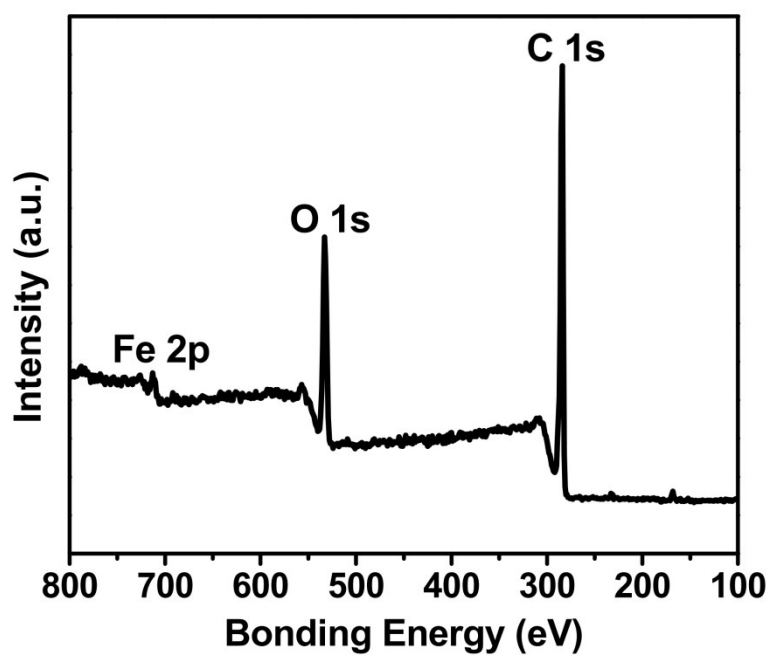


Fig. S2 The XPS result of Fe-BaP.

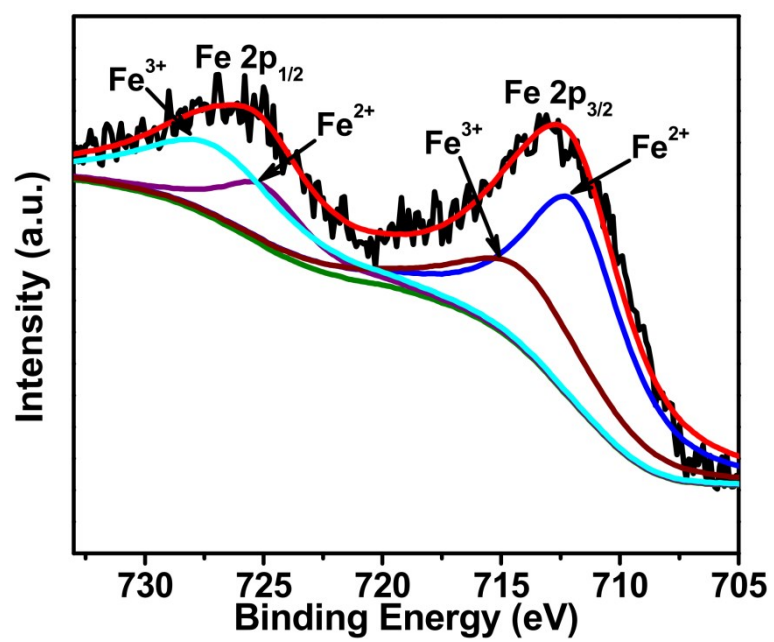


Fig. S3 XPS spectra for Fe 2p.

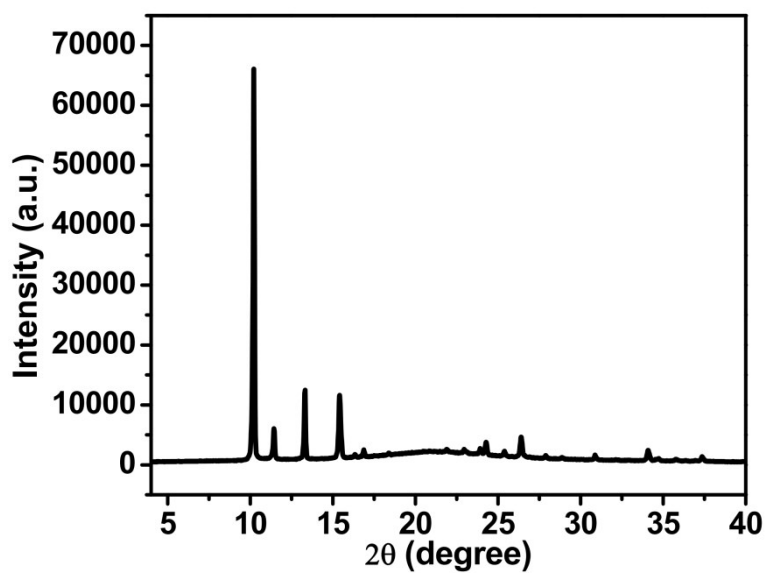


Fig. S4 The PXRD pattern of baicalein.

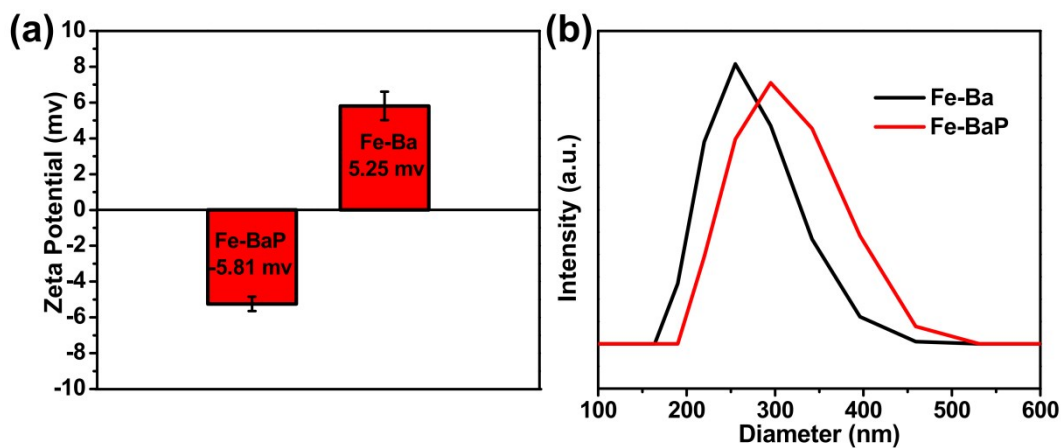


Fig. S5 The zeta potential and DLS results of Fe-Ba and Fe-BaP.

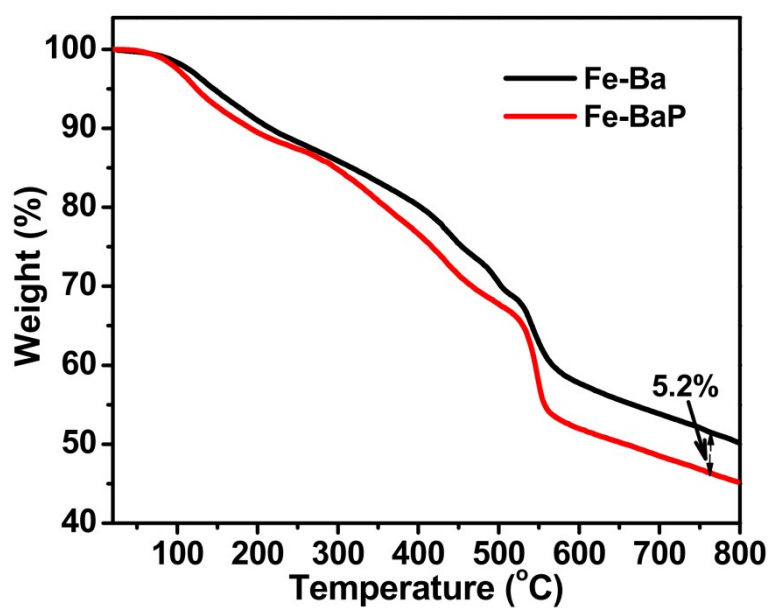


Fig. S6 TGA curves of Fe-Ba and Fe-BaP.

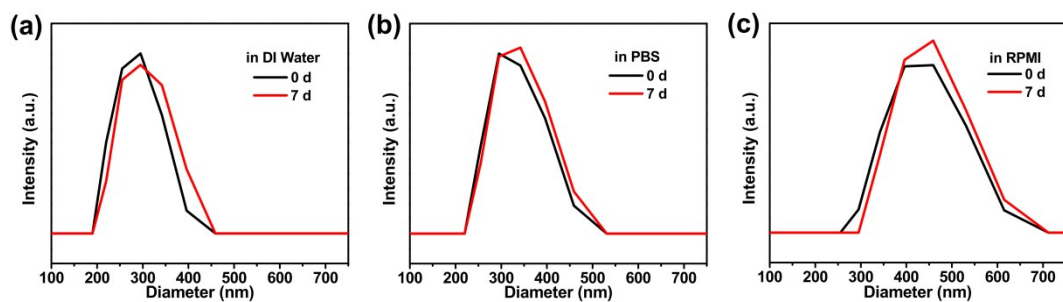


Fig. S7 The DLS results of Fe-BaP dispersed in (a) H₂O, (b) PBS and (c) RPMI, respectively.



Fig. S8 The photographs of CFAP dispersed in H₂O, PBS, and RPMI, respectively.



Fig. S9 Photographs of baicalein (left) and the as-synthesized Fe-BaP (right) in ethanol.

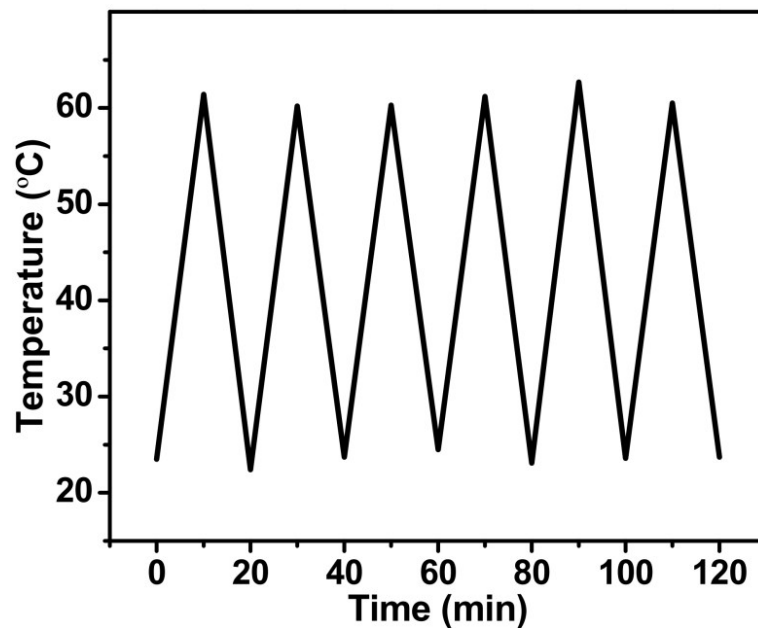


Fig. S10 Photostability test of Fe-BaP aqueous solution with a concentration of $150 \mu\text{g mL}^{-1}$.

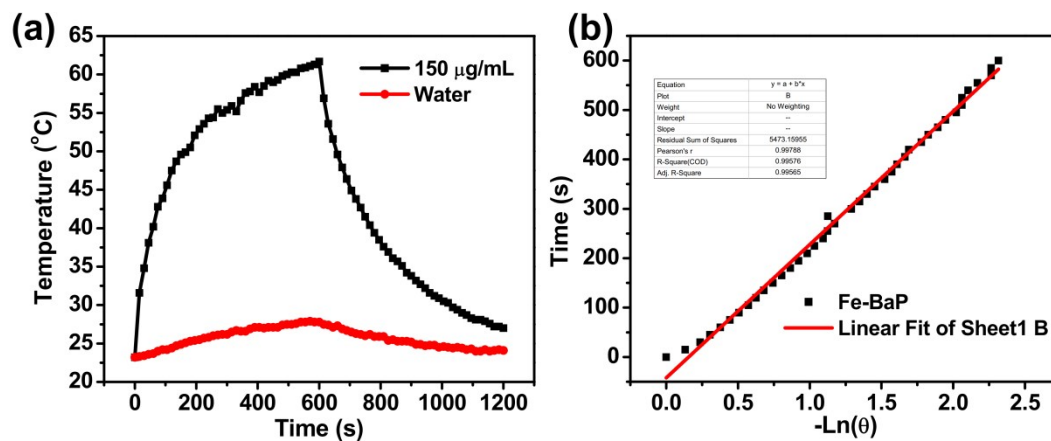


Fig. S11 (a) Photothermal effect of Fe-PAP aqueous solution ($150 \mu\text{g mL}^{-1}$) irradiated with an 808 nm laser for 10 min (1.3 W cm^{-2}). (b) Linear fit of time/ $-\ln(\theta)$ obtained during the cooling process.

Table S1 Photothermal conversion efficiency of Fe-BaP.

A_{808}	$T_{\max}-T_{\text{sur}}$	T_s	η
1.24	38.5	269.733	45.6%

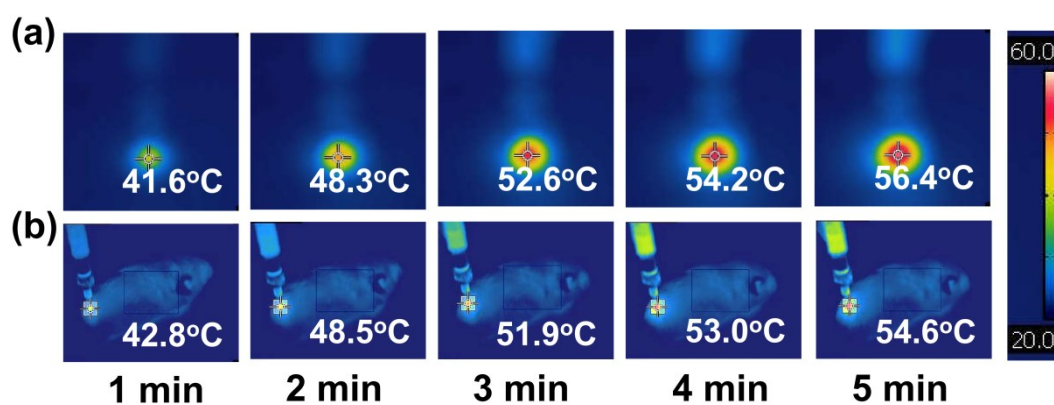


Fig. S12 The (a) Fe-BaP aqueous solution and (d) tumor-bearing mouse after injection with Fe-BaP under laser irradiation ($150 \mu\text{g mL}^{-1}$, 1.3 W cm^{-1}).

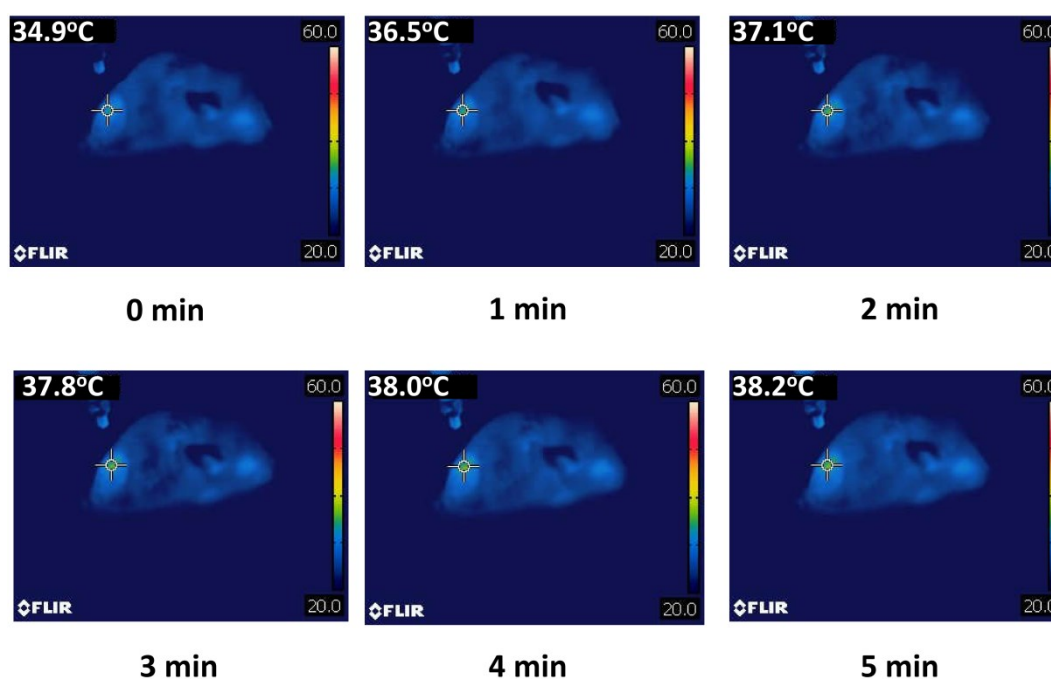


Fig. S13 The infrared thermal images of tumor-bearing mouse after injection with PBS under 808 nm laser irradiation ($150 \mu\text{g mL}^{-1}$, 1.3 W cm^{-1}).

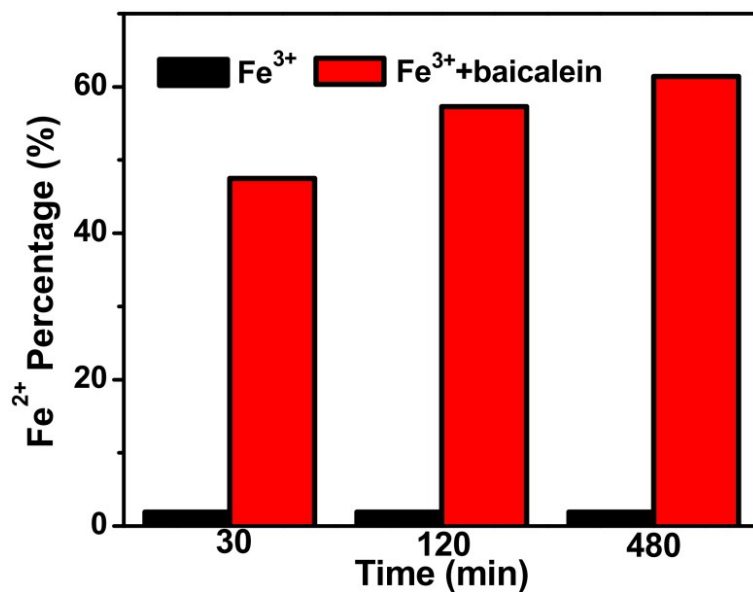


Fig. S14 Detection of Fe²⁺ after treatment with Fe³⁺ and Fe³⁺+ baicalein, respectively.

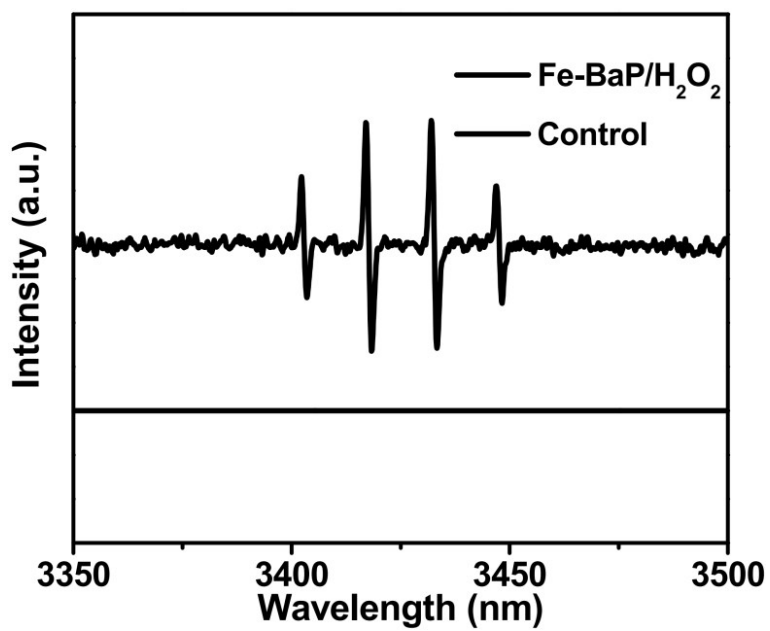


Fig. S15 EPR spectra of Fe-BaP.

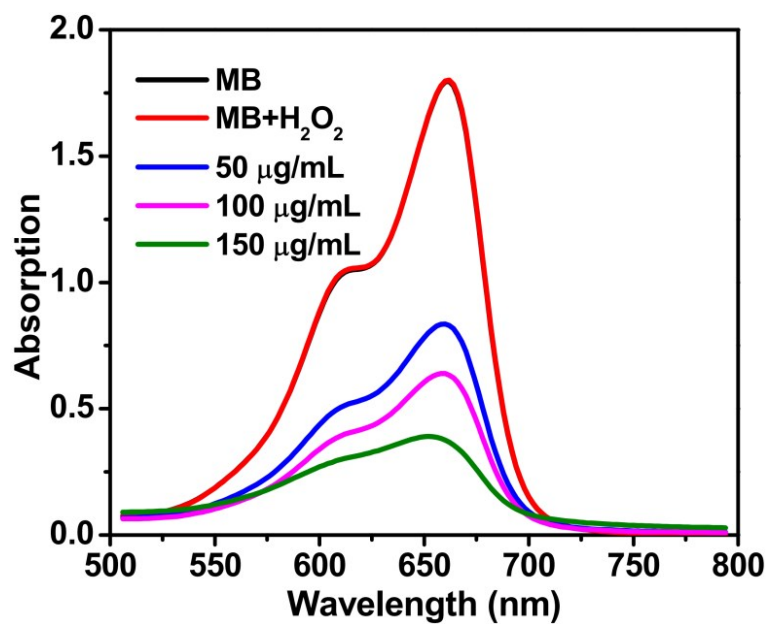


Fig. S16 UV-vis spectra of MB + H₂O₂ under different Fe-BaP concentrations at room temperature (the reaction time was 5 min).

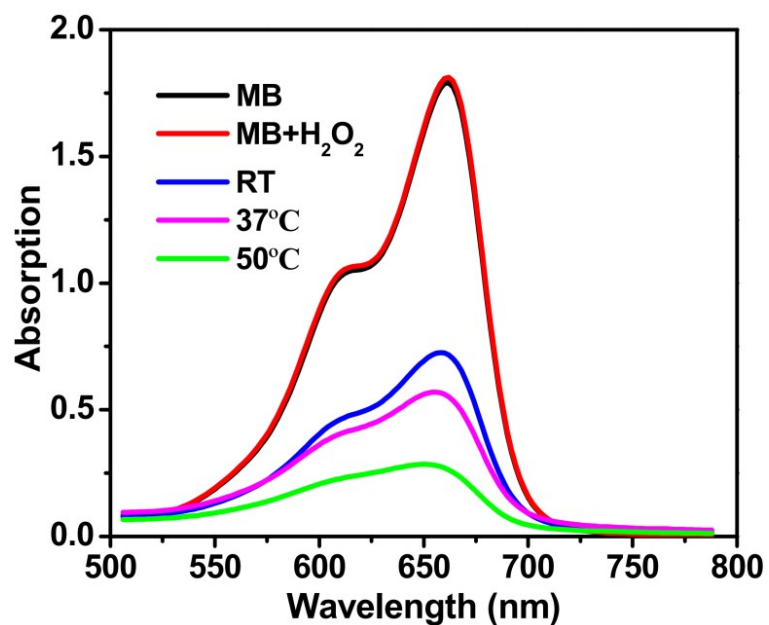


Fig. S17 UV-vis spectra of MB + H₂O₂ in the presence of 50 µg mL⁻¹ Fe-BaP under different temperatures (the reaction time was 5 min).

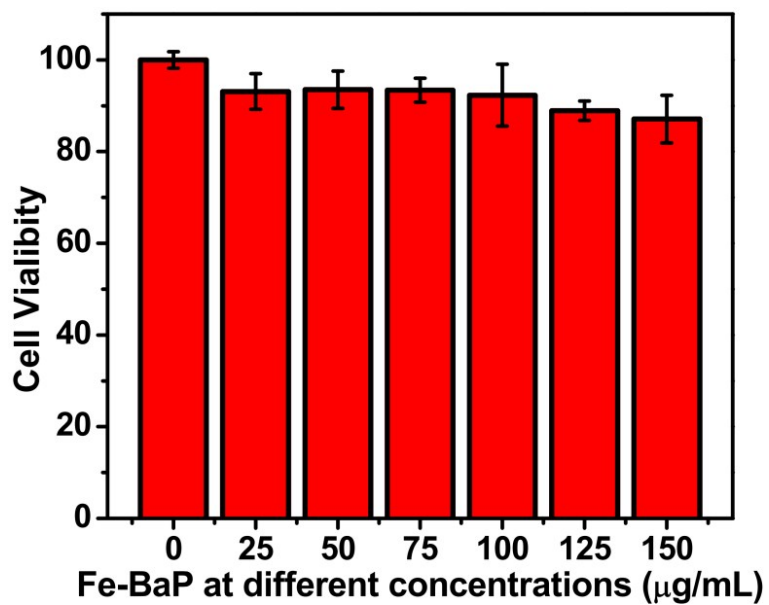


Fig. S18 In vitro cell viability test against L929 cells incubated with different concentrations of Fe-BaP.

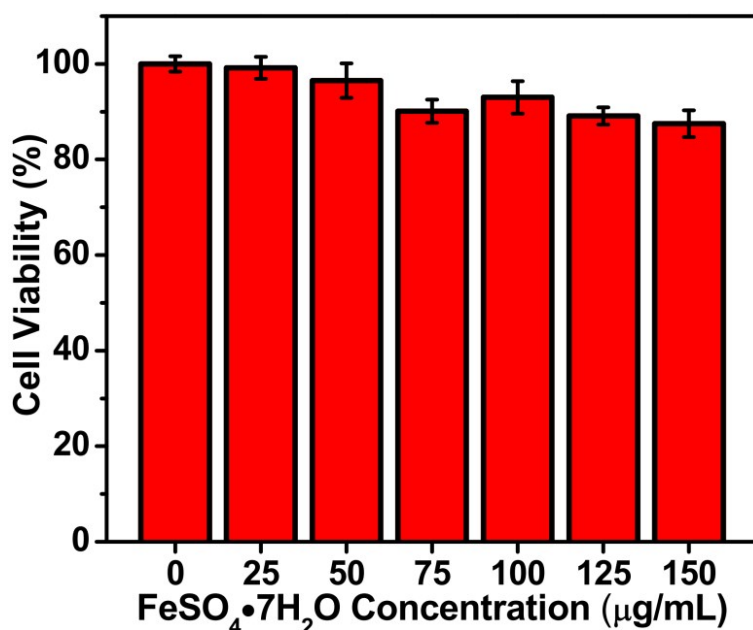


Fig. S19 In vitro cell viability test against 4T1 cells incubated with FeSO₄·7H₂O for different concentrations.

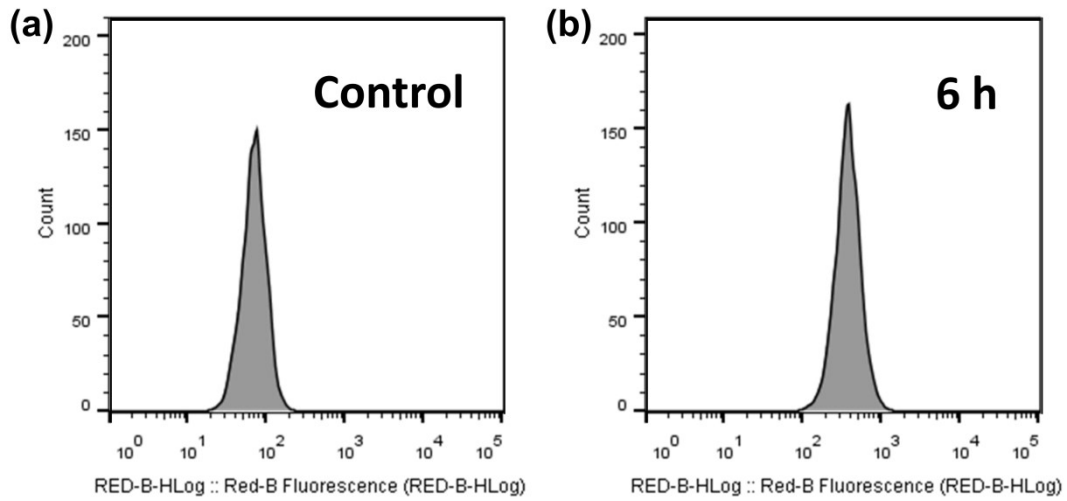


Fig. S20 Flow cytometry of 4T1 cells treated with Fe-BaP NPs for 6 h.

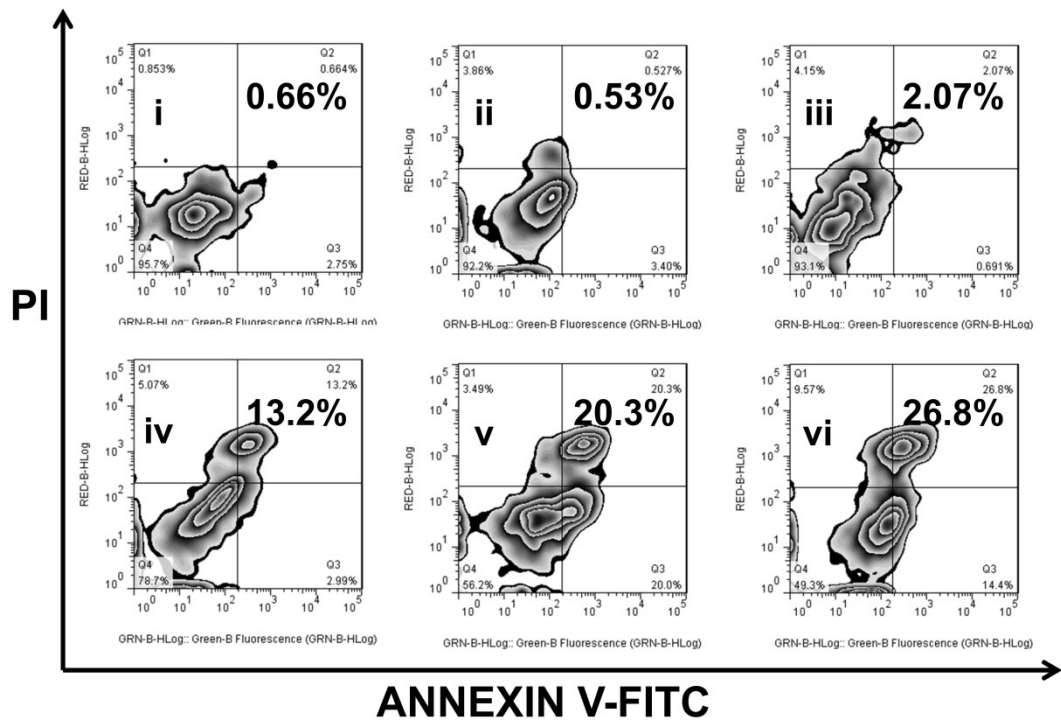


Fig. S21 Flow cytometry data for apoptosis of 4T1 cells treated with (i) PBS, (ii) PBS + NIR, (iii) Fe-BaP, (iv) Fe-BaP + 100 μ M H₂O₂, (v) Fe-BaP + NIR, and (vi) Fe-BaP + 100 μ M H₂O₂ + NIR, respectively. The concentration of Fe-BaP is 150 μ g mL⁻¹ and laser irradiation conditions are 0.9 W cm⁻² and 808 nm.

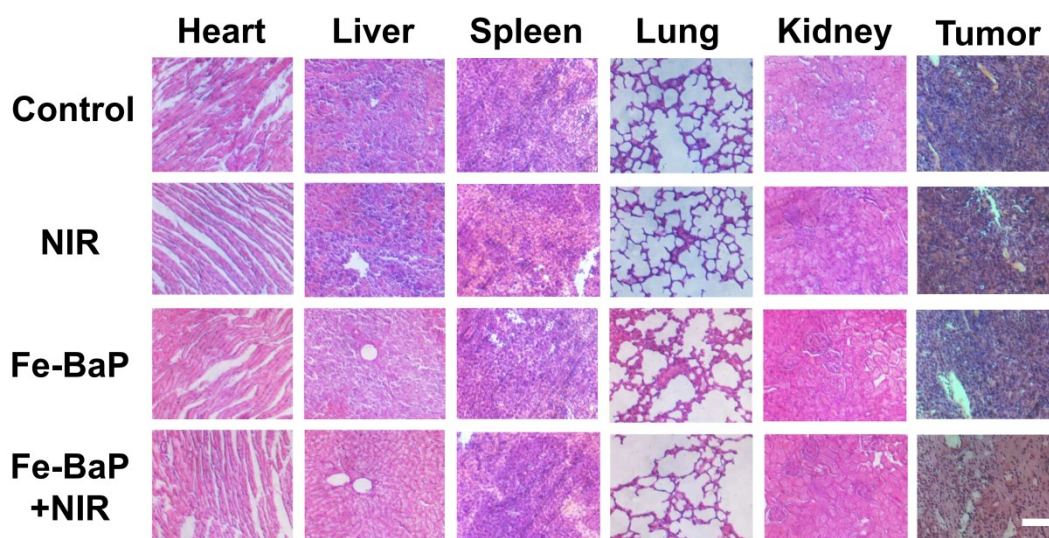


Fig. 22 H&E stained images of the major organs and tumor issues sections of mice after different treatments. Scar bar: 40 μm .

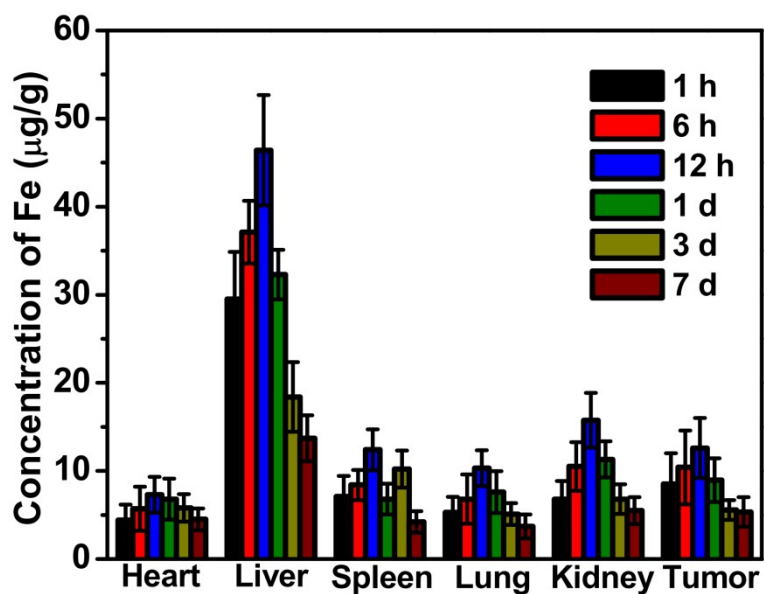


Fig. 23 The in vivo biodistribution of Fe-BaP nanoparticles.